

Exact Analytical Solution for Fields in a Lossy Cylindrical Structure with Linear Gradient Index Metamaterials

Mariana Dalarsson^{1, *}, Martin Norgren¹, and Zoran Jaksic²

Abstract—We investigate the electromagnetic wave propagation across a finite inhomogeneous and anisotropic cylindrical metamaterial composite containing both positive and negative effective refractive index parts with linear spatial gradient. Exact analytical solutions for the electric and magnetic field distributions are obtained for a linear variation of effective refractive index across the structure. The exact analytical results for the electric and magnetic fields are compared to the numerical results obtained using the numerical simulation software HFSS. The model allows for general temporal dispersion and uniform losses within the composite.

1. INTRODUCTION

In the present paper, we study the electromagnetic wave propagation through cylindrical structures including artificial material composites, with electromagnetic properties not readily found in nature, usually called metamaterials (MM). In particular, we are interested in a special class of MMs, the left-handed materials (LHM), theoretically described by Veselago in 1967 [1]. The first practical implementations of LHM were proposed by Pendry et al. [2, 3]. LHM are produced as arrays of subwavelength structural units (“particles”) with negative effective relative permittivity and permeability. First LHM-“particles” were split-ring resonators and nanowires, providing negative permeability and permittivity of the composites [3]. Other frequently used LHM-“particles” include complementary split-ring resonators [4], cut-wire pairs/plate pairs [5] and double fishnets [6, 7, 8]. The first experimental confirmation of LHM-properties in the microwave range of frequencies was reported in [9], and the experimental fishnet-type LHM in the visible range of frequencies was reported in [10].

Based on the specific properties of LHM, such as the negative index of refraction, radiation tension instead of pressure, inverse Doppler effect etc. [11, 12] a number of potential applications have been proposed and studied. These include superlenses/hyperlenses enabling imaging far below the diffraction limit [13, 14], waveguides and resonant cavities with dimensions orders of magnitude smaller than the operating wavelength [15], invisibility cloaks and transformation optics [16] etc..

The above-mentioned studies usually consider structures with constant effective permittivity and permeability within the LHM part and abrupt transitions to the surrounding “right-handed media” (RHM). However, there is a growing theoretical and practical interest in composites with gradual spatially varying effective permittivity and permeability between LHM and RHM as well as within the LHM structure. Graded refractive index is of interest for both transformation optics including hyperlenses [17] and invisibility cloaks [18]. Other proposed applications of graded metamaterials include beam shaping and directing, enhancement of nonlinear effects [19], superlenses [20], etc.

The first paper dedicated to gradient refractive index LHM was published in 2005 [21]. Analytical approaches to graded index metamaterial structures are of special interest, since they ensure fast, simple

Received 20 April 2015, Accepted 5 May 2015, Scheduled 11 May 2015

* Corresponding author: Mariana Dalarsson (mardal@kth.se).

¹ Department of Electromagnetic Engineering, Royal Institute of Technology, Stockholm, Sweden. ² Center of Microelectronic Technologies and Single Crystals, Institute of Chemistry, Technology and Metallurgy, University of Belgrade, Belgrade, Serbia.

and direct route to the determination of the field distribution and the calculation of the scattering parameters within such materials [22, 28].

The LHM structures with gradient index are of importance for transformation optics [29, 30], the most well-known example being the invisibility cloaks. For instance, optical carpet cloaks [31] were reported with effective index gradient obtained by drilling hole arrays with varying geometry [32]. Other important applications include optical and generally electromagnetic concentrators based on metamaterials, beam shapers and beam steering devices, as well as different kinds of metamaterial lenses, including hyperlenses [17], for the transformation of near field into the far field. Finally, an important application is gradient index circuitry utilizing metamaterial waveguides [33].

The present study is a generalization of our previous work [25–28] to coaxial cylindrical structures with radial propagation of the electromagnetic wave. We present an exact analytical solution of Helmholtz' equations for the radial propagation of electromagnetic waves through a lossy linear gradient-index RHM-LHM composite, and compare the results with the corresponding results obtained using the simulation software ANSYS HFSS.

2. PROBLEM FORMULATION

The geometry of the present problem is shown in Fig. 1. We assume that there is a metallic cylindrical antenna of radius a which transmits the plane electromagnetic waves in the radial direction. The electric field points in the azimuthal angular φ -direction and has the form $\vec{E} = E(r)\vec{e}_\varphi$, while the magnetic field points in the z -direction and has the form $\vec{H} = H(r)\vec{e}_z$. The wave propagates along the radial r -direction. Around the emitting metallic antenna there is a coaxial layer of gradient index LHM of radial thickness a . Around the LHM-layer, there is a coaxial layer of gradient index RHM of the same radial thickness a . The structure is enclosed by a metallic cylinder at the radius $3a$. For the sake of simplicity, in the present paper we assume that both LHM and RHM layers are of the same thickness a being equal to the radius of the inner metallic cylinder. This does not imply any loss of generality, since the exact analytical results are available for any radii of the metallic boundaries and any thicknesses of the LHM and RHM layers. In principle, one could choose the diameter of the outer boundary as very large compared to the diameter of the thin-wire inner boundary, such that the present model can be applied also to situations of fields far away from the emitting structure. Furthermore, we assume that the boundary effects in the axial direction (along the z -axis) can be neglected, such that any fields generated by these boundary effects are much smaller than the fields radiated by the inner cylinder.

The spatial variation of the refractive index along the radial direction is described by a linear function. Maxwell equations in cylindrical coordinates for our coaxial composite are of the following

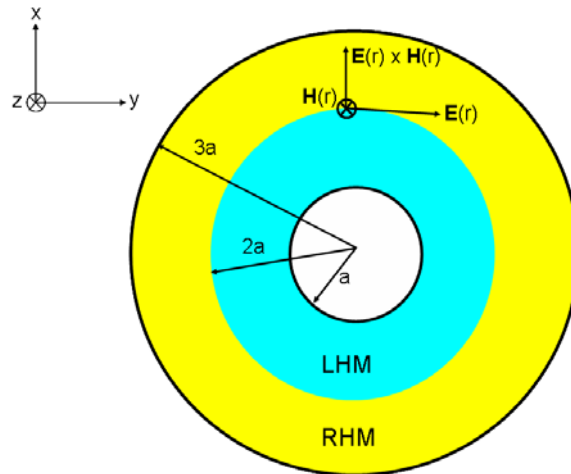


Figure 1. Propagation of an electromagnetic wave through a finite coaxial cylindrical graded index structure with a linear profile.

form

$$\frac{1}{r} \frac{d}{dr} [rE(r)] = -j\omega\mu(r)H(r), \quad \frac{dH}{dr} = -j\omega\epsilon(r)E(r). \quad (1)$$

From the Maxwell Equation (1) it is possible to eliminate either $E(r)$ or $H(r)$ to obtain the following two Helmholtz equations for $H(r)$ and $E(r)$ respectively

$$\frac{d^2 H}{dr^2} - \frac{1}{\left(\frac{\epsilon}{r}\right)} \frac{d}{dr} \left(\frac{\epsilon}{r}\right) \frac{dH}{dr} + \omega^2 \mu \epsilon H = 0, \quad \frac{d^2}{dr^2} (rE) - \frac{1}{(\mu r)} \frac{d(\mu r)}{dr} \frac{d}{dr} (rE) + \omega^2 \mu \epsilon (rE) = 0. \quad (2)$$

where $\epsilon = \epsilon(\omega, r)$ and $\mu = \mu(\omega, r)$ are the frequency-dependent dielectric permittivity and magnetic permeability, respectively. The spatial dependency of the functions $\epsilon(r)$ and $\mu(r)$ may be completely arbitrary. The only limit of applicability of the present approach, in terms of wavelength of the radiation versus the structural period of the metamaterial, is posed by the requirement that the effective medium approximation remains valid, i.e., that the structure periodicity is much smaller than the operating wavelength.

3. ANALYTICAL SOLUTIONS OF FIELD EQUATIONS

Let us now consider a finite and inhomogeneous periodic structure, where the real parts of the effective dielectric permittivity and magnetic permeability vary from negative values (LHM) to positive values (RHM) as suitably chosen functions to ensure the linear gradient of the refractive index. The thickness a of the LHM part is equal to that of the RHM part. In the present paper we use the following permittivity and permeability functions

$$\epsilon(\omega, r) = \left[\epsilon_0 \epsilon_R(\omega) \frac{r - 2a}{a} - j\epsilon_0 \epsilon_I(\omega) \right] \frac{r}{a}, \quad \mu(\omega, r) = \left[\mu_0 \mu_R(\omega) \frac{r - 2a}{a} - j\mu_0 \mu_I(\omega) \right] \frac{a}{r}. \quad (3)$$

where $-\epsilon_R(\omega)$ and $-\mu_R(\omega)$ are the frequency dependent real parts of the effective permittivity and permeability in the LHM material just outside $r = a$, respectively. Analogously, $\epsilon_I(\omega)$ and $\mu_I(\omega)$ are the imaginary parts of the effective permittivity and permeability in the LHM material just outside $r = a$, respectively. An example of the spatial dependence of the real parts of the two functions $\epsilon = \epsilon(\omega, r)$ and $\mu = \mu(\omega, r)$ is shown in Fig. 2. For a material to be passive, i.e., without gain, and to satisfy causality, the imaginary parts of both the permittivity and permeability must be positive. Otherwise, the model is valid for arbitrary temporal dispersion and losses as long as the general mathematical and physical constraints are satisfied (e.g., Kramers-Kronig relations). From the definitions (3) we readily see that the present choices of the effective permittivity and permeability functions are such that the functions (ϵ/r) and (μr) occurring in the Helmholtz Equation (2) respectively are indeed linear functions.

Practical realization of the functions $\epsilon = \epsilon(\omega, r)$ and $\mu = \mu(\omega, r)$, shown in Fig. 2, can be done using thin layers of LHM and RHM in the coaxial cylindrical structure shown in Fig. 1. Examples of

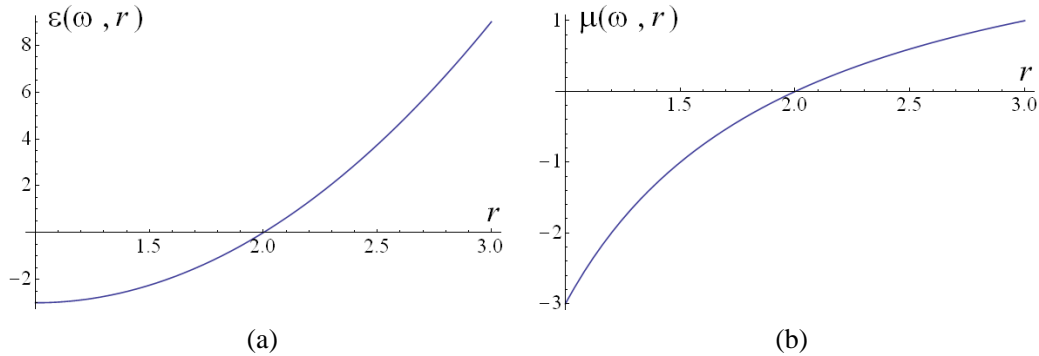


Figure 2. Example of the real parts of the functions, (a) $\epsilon = \epsilon(\omega, r)$ and (b) $\mu = \mu(\omega, r)$.

structures that actually exploit the layered approach to inhomogeneity, in the context of GRIN lenses, can be found in, e.g., [34, 35]. The practical realization approach to be used in the present study would typically be similar to that described in these papers, and references therein. Following the approach adopted in [26–28], we also require that the real and imaginary parts of the effective permittivity and permeability satisfy the condition

$$\frac{\mu_I(\omega)}{\mu_R(\omega)} = \frac{\epsilon_I(\omega)}{\epsilon_R(\omega)} = \beta(\omega). \quad (4)$$

The condition (4) is a restrictive mathematical requirement on the complex permittivity and permeability that reduces our analysis to a special case. A justification for the requirement (4) is based on the fact that both permittivity and permeability of a significant part of LHM structures reported until now can be described by Drude or Lorentz models, i.e., that $\epsilon(\omega)$ and $\mu(\omega)$ are strongly resonant and thus quite narrowband. In order to obtain the widest possible frequency range of negative refractive index, it is then useful to have the best possible overlap between the ranges of negative values of real parts of $\epsilon(\omega)$ and $\mu(\omega)$. In an ideal situation their dispersions in the resonant range would be therefore identical. On the other hand, in order to preserve causality, the imaginary parts of both $\epsilon(\omega)$ and $\mu(\omega)$ must be positive and their dispersions are determined by the real parts. Thus the imaginary parts should also overlap. Actually (4) can be seen as a condition, although very stringent, for the maximum bandwidth of Drude- or Lorentz-type resonant LHM structures. Using (4), we readily obtain

$$\epsilon(\omega, r) = \epsilon_0 \epsilon_R(\omega) \left[\frac{r - 2a}{a} - j\beta \right] \frac{r}{a}, \quad \mu(\omega, r) = \mu_0 \mu_R(\omega) \left[\frac{r - 2a}{a} - j\beta \right] \frac{a}{r}. \quad (5)$$

Except for the condition (4), our method allows for arbitrary temporal dispersion. Upon the condition (4), the inverse of the wave impedance $Z(\omega, r)$ as well as the refractive index $n(\omega, r)$ become

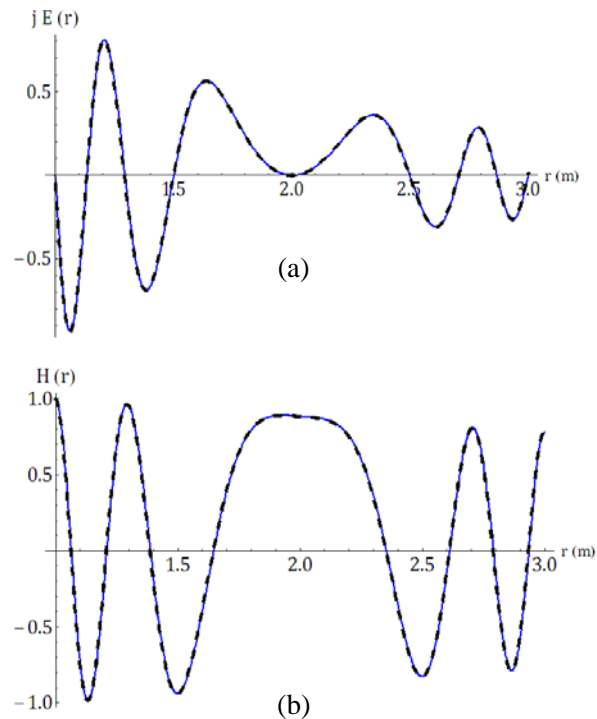


Figure 3. Comparison of the analytical (full line) and numerical (dashed line) results for the amplitudes of (a) electric field $E(r)$ and (b) magnetic field $H(r)$, with $E_0 = 1$, $H_0 = 1$, $a = 1$ m, $k = 8\pi$ 1/m and $\beta = 0.5 \times 10^{-2}$.

linear spatial functions throughout the entire structure

$$\frac{1}{Z(\omega, r)} = \sqrt{\frac{\epsilon(\omega, r)}{\mu(\omega, r)}} = \sqrt{\frac{\epsilon_0 \epsilon_R(\omega)}{\mu_0 \mu_R(\omega)}} \frac{r}{a}, \tag{6}$$

$$n(\omega, r) = c\sqrt{\epsilon(\omega, r)\mu(\omega, r)} = \sqrt{\epsilon_R(\omega)\mu_R(\omega)} \left[\frac{r - 2a}{a} - j\beta \right]. \tag{7}$$

The Equation (2), with $\epsilon = \epsilon(\omega, r)$ and $\mu = \mu(\omega, r)$ given by (5), allow for exact analytic solutions of the form

$$rE(r) = -jaE_0e^{-\beta k(r-a)} \sin \left[\frac{kr}{2a}(r - 4a) + \frac{3ka}{2} \right], \quad H(r) = H_0e^{-\beta k(r-a)} \cos \left[\frac{kr}{2a}(r - 4a) + \frac{3ka}{2} \right] \tag{8}$$

where $H_0 = H(a)$ is the amplitude of the emitted magnetic field strength at the inner cylinder (antenna) surface $r = a$, and E_0 is the emitted electric field strength defined by $E_0 = Z(a)H_0$. The wave number k is defined by $k(\omega) = \sqrt{\epsilon_0\mu_0\epsilon_R(\omega)\mu_R(\omega)}$.

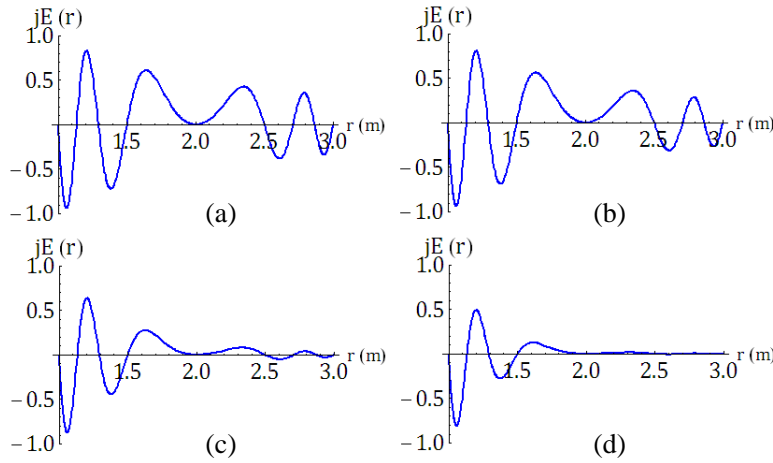


Figure 4. Amplitudes of the electric field $E(r)$, with $E_0 = 1$ $a = 1$ m, $k = 8\pi$ /m, (a) $\beta = 0$, (b) $\beta = 0.5 \times 10^{-2}$, (c) $\beta = 0.5 \times 10^{-1}$, and (d) $\beta = 10^{-1}$.

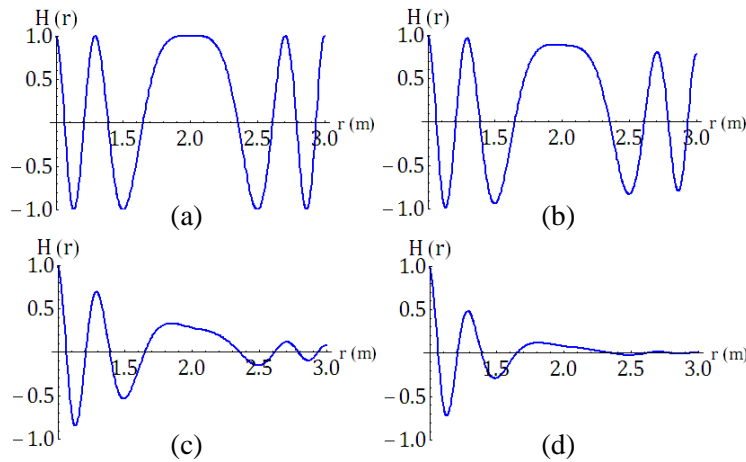


Figure 5. Amplitudes of the magnetic field $H(r)$, with $H_0 = 1$, $a = 1$ m, $k = 8\pi$ /m, (a) $\beta = 0$, (b) $\beta = 0.5 \times 10^{-2}$, (c) $\beta = 0.5 \times 10^{-1}$, and (d) $\beta = 10^{-1}$.

4. RESULTS AND DISCUSSION

The amplitudes of the exact analytical solutions (full lines) for the electric field $E(r)$ and magnetic field $H(r)$, given by Eq. (8), are compared to the corresponding numerical solutions (dashed lines) in Figs. 3(a) and 3(b) respectively. From Figs. 3(a) and 3(b) we see that there is an excellent agreement between the exact analytical results (full lines) and the corresponding numerical results (dashed lines), as expected. In Figs. 3(a) and 3(b) we also see the expected phase change, indicating the change of the direction of the wave vector [24–28] at the boundary between LHM and RHM at $r = 2a$. Furthermore, we note that the tangential electric field $E(r)$ satisfies the usual boundary conditions on the metallic boundaries at $r = a$ and $r = 3a$ where it becomes equal to zero.

The dependencies of the amplitudes for the electric field $E(r)$ and magnetic field $H(r)$, given by Eq. (8), on the loss parameter β are illustrated in Figs. 4 and 5, respectively. From Figs. 4 and 5 we see that the attenuation of the field amplitudes increases with increasing loss factor β as expected. The dependencies of the amplitudes for the electric field $E(r)$ and magnetic field $H(r)$, given by Eq. (8), on the permittivity and permeability, i.e., on the wave number parameter k , are illustrated in Figs. 6 and 7, respectively. From Figs. 6 and 7 we see that the field amplitudes display shorter wavelengths with

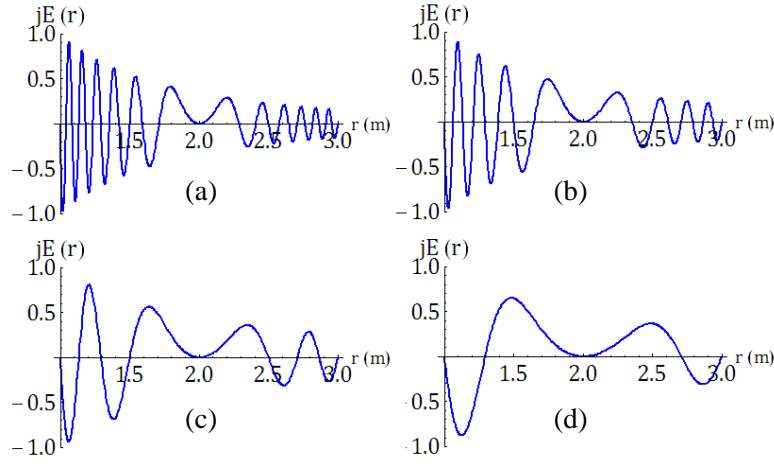


Figure 6. Amplitudes of the electric field $E(r)$, with $E_0 = 1$, $a = 1$ m, $\beta = 0.5 \times 10^{-2}$, (a) $k = 24\pi$ 1/m, (b) $k = 16\pi$ 1/m, (c) $k = 8\pi$ 1/m, and (d) $k = 4\pi$ 1/m.

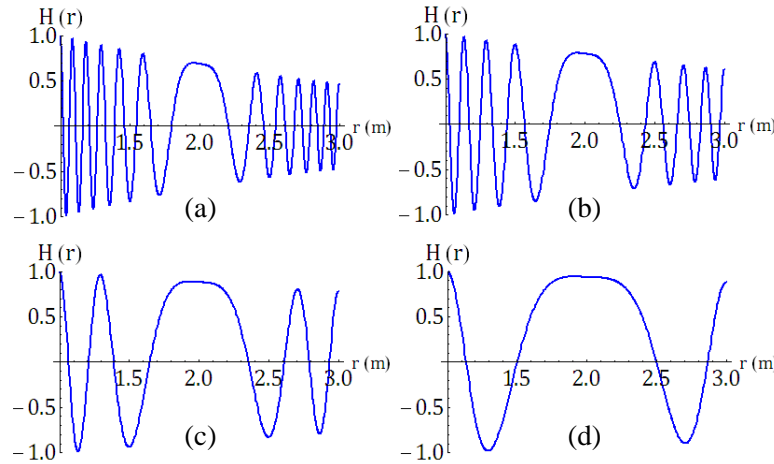


Figure 7. Amplitudes of the magnetic field $H(r)$, with $H_0 = 1$, $a = 1$ m, $\beta = 0.5 \times 10^{-2}$, (a) $k = 24\pi$ 1/m, (b) $k = 16\pi$ 1/m, (c) $k = 8\pi$ 1/m, and (d) $k = 4\pi$ 1/m.

increasing wave number factor k as expected. Furthermore the phase change, indicating the change of the direction of the wave vector [24–28] at the boundary between LHM and RHM at $r = 2a$, becomes even more distinct for the waves with higher k .

5. CONCLUSIONS

We obtained the exact analytical solutions of the Helmholtz equations for radial electromagnetic wave propagation through a coaxial cylindrical structure with radially graded permittivity and permeability profiles changing along the direction of propagation. We compared these results with the corresponding numerical results obtained using the standard numerical simulation software ANSYS HFSS, whereby we obtained an excellent agreement between the analytical and numerical results. The model is valid for arbitrary temporal dispersion and arbitrary losses, as long as the general mathematical and physical constraints are satisfied. The exact analytical results are available for any radii of the metallic boundaries and any thicknesses of the LHM and RHM layers. In principle, one can choose the diameter of the outer boundary as very large compared to the diameter of the thin-wire inner boundary, such that the present model can be applied also to situations of fields far away from the emitting structure. We analyzed a special case of a linear model of the refractive index gradient. The present study can be extended to a number of other practical axially symmetric geometries, and to a number of other models of the refractive index gradient (notably hyperbolic tangent functions or periodic trigonometric functions). Such studies will be a part of our continued efforts.

ACKNOWLEDGMENT

Work of Z. J. was partially funded by the Serbian Ministry of Education, Science and Technological Development through the project TR32008 MiNaSyS Micro and Nanosystems for Power Engineering, Process Industry and Environmental Protection.

REFERENCES

1. Veselago, V. G., “The electrodynamics of substances with simultaneously negative values of ϵ and μ ,” *Sov. Phys. Uspekhi*, Vol. 10, 509–514, 1968, Doi: 10.1070/PU1968v010n04ABEH003699.
2. Pendry, J. B., A. J. Holden, D. J. Robbins, and W. J. Stewart, “Low frequency plasmons in thin-wire structures,” *J. Phys. — Condens. Mat.*, Vol. 10, 4785–4809, 1998, Doi: 10.1088/0953-8984/10/22/007.
3. Pendry, J. B., A. J. Holden, D. J. Robbins, and W. J. Stewart, “Magnetism from conductors and enhanced nonlinear phenomena,” *IEEE T. Microw. Theory*, Vol. 47, 2075–2084, 1998, Doi: 10.1088/0953-8984/10/22/007.
4. Falcone, F., T. Lopetegui, M. A. G. Laso, J. D. Baena, J. Bonache, M. Beruete, R. Marques, F. Martin, and M. Sorolla, “Babinet principle applied to the design of metasurfaces and metamaterials,” *Phys. Rev. Lett.*, Vol. 93, No. 19, 197401-1–4, 2004, Doi: 10.1103/PhysRevLett.93.197401.
5. Dolling, G., C. Enkrich, M. Wegener, J. F. Zhou, C. M. Soukoulis, and S. Linden, “Cut-wire pairs and plate pairs as magnetic atoms for optical metamaterials,” *Opt. Lett.*, Vol. 30, 3198–3200, 2005, Doi: 10.1364/OL.30.003198.
6. Zhang, S., W. Fan, N. C. Panou, K. J. Malloy, R. M. Osgood, and S. R. J. Brueck, “Experimental demonstration of near-infrared negative-index metamaterials,” *Phys. Rev. Lett.*, Vol. 95, No. 13, 137404-1–4, 2005, Doi: 10.1103/PhysRevLett.95.137404.
7. Kafesaki, M., I. Tsiapa, N. Katsarakis, T. Koschny, C. M. Soukoulis, and E. N. Economou, “Left-handed metamaterials: The fishnet structure and its variations,” *Phys. Rev. B*, Vol. 75, 235114-1–9, 2007, Doi: 10.1103/PhysRevB.75.235114.
8. Valentine, J., S. Zhang, T. Zentgraf, E. Ulin-Avila, D. A. Genov, G. Bartal, and X. Zhang, “Three-dimensional optical metamaterial with a negative refractive index,” *Nature*, Vol. 455, 376–379, 2008, Doi: 10.1038/nature07247.

9. Shelby, R. A., D. R. Smith, and S. Schultz, "Experimental verification of a negative index of refraction," *Science*, Vol. 292, 77–79, 2001, Doi: 10.1126/science.1058847.
10. Xiao, S., U. K. Chettiar, A. V. Kildishev, V. P. Drachev, and V. M. Shalaev, "Yellow-light negative-index metamaterials," *Opt. Lett.*, Vol. 34, 3478–3480, 2009, Doi: 10.1364/OL.34.003478.
11. Cai, W. and V. M. Shalaev, *Optical Metamaterials: Fundamentals and Applications*, Springer, Dordrecht, 2009, doi:10.1007/978-1-4419-1151-3.
12. Ramakrishna, S. A. and T. M. Grzegorzczak, *Physics and Applications of Negative Refractive Index Materials*, SPIE Press, Bellingham, WA & CRC Press, Taylor & Francis Group, Boca Raton FL, 2009, Doi: 10.1080/00107510903257459.
13. Pendry, J. B., "Negative refraction makes a perfect lens," *Phys. Rev. Lett.*, Vol. 85, 3966–3969, 2000. Doi: 10.1103/PhysRevLett.85.3966.
14. Fang, N., H. Lee, C. Sun, and X. Zhang, "Sub-diffraction-limited optical imaging with a silver superlens," *Science*, Vol. 308, 534–537, 2005, Doi: 10.1126/science.1108759.
15. Engheta, N., "An idea for thin subwavelength cavity resonators using metamaterials with negative permittivity and permeability," *IEEE Anten. Wirel. Propag. Lett.*, Vol. 1, 10–13, 2002, Doi: 10.1109/LAWP.2002.802576.
16. Pendry, J. B., D. Shurig, and D. R. Smith, "Controlling electromagnetic fields," *Science*, Vol. 312, 1780–1782, 2006, Doi: 10.1126/science.1126493.
17. Jacob, Z., L. V. Alekseyev, and E. Nerimanov, "Optical hyperlens: Far-field imaging beyond the diffraction limit," *Opt. Express*, Vol. 14, 8247–8256, 2006, Doi: 10.1364/OE.14.008247.
18. Cai, W., U. K. Chettiar, A. V. Kildishev, and V. M. Shalaev, "Optical cloaking with metamaterials," *Nat. Photonics*, Vol. 1, 224–227, 2007, Doi: 10.1038/nphoton.2007.28..
19. Fung, T. H., L. L. Leung, J. J. Xiao, and K. W. Yu, "Controlling electric fields spatially by graded metamaterials: Implication on enhanced nonlinear optical responses," *Opt. Commun.*, Vol. 282, 1028–1031, 2009, Doi: 10.1016/j.optcom.2008.11.028..
20. Ramakrishna, S. A. and J. B. Pendry, "Spherical perfect lens: Solutions of Maxwell's equations for spherical geometry," *Phys. Rev. B*, Vol. 69, 115115–1–7, 2004, Doi: 10.1103/PhysRevB.69.115115.
21. Smith, D. R., J. J. Mock, A. F. Starr, and D. Schurig, "Gradient index metamaterials," *Phys. Rev. E*, Vol. 71, 036609–1–6, 2005, Doi: 10.1103/PhysRevE.71.036609.
22. Pinchuk, A. O. and G. C. Schatz, "Metamaterials with gradient negative index of refraction," *J. Opt. Soc. Am. A*, Vol. 24, A39–A44, 2007. Doi: 10.1364/JOSAA.24.000A39.
23. Litchinitser, N. M., A. I. Maimistov, I. R. Gabitov, R. Z. Sagdeev, and V. M. Shalaev, "Metamaterials: Electromagnetic enhancement at zero-index transition," *Opt. Lett.*, Vol. 33, 2350–2352, 2008, Doi: 10.1364/OL.33.002350.
24. Dalarsson, M. and P. Tassin, "Analytical solution for wave propagation through a graded index interface between a right-handed and a left-handed material," *Opt. Express*, Vol. 17, No. 8, 6747–6752, 2009, Doi: 10.1364/OE.17.006747.
25. Dalarsson, M., M. Norgren, and Z. Jaksic, "Lossy gradient index metamaterial with sinusoidal periodicity of refractive index: Case of constant impedance throughout the structure," *J. Nanophotonics*, Vol. 5, No. 1, 051804–1–8, 2011, Doi: 10.1117/1.3590251.
26. Dalarsson, M., M. Norgren, N. Doncov, and Z. Jaksic, "Lossy gradient index transmission optics with arbitrary periodic permittivity and permeability and constant impedance throughout the structure," *J. Opt.*, Vol. 14, No. 6, 065102–1–7, 2012, Doi: 10.1088/2040-8978/14/6/065102.
27. Dalarsson, M., M. Norgren, T. Asenov, N. Doncov, and Z. Jaksic, "Exact analytical solution for fields in gradient index metamaterials with different loss factors in negative and positive refractive index segments," *J. Nanophotonics*, Vol. 7, No. 1, 073086–1–13, 2013, Doi: 10.1117/1.JNP.7.073086.
28. Dalarsson, M., M. Norgren, T. Asenov, and N. Doncov, "Arbitrary loss factors in the wave propagation between RHM and LHM media with constant impedance throughout the structure," *Progress In Electromagnetics Research*, Vol. 137, 527–538, 2013.
29. Mei, Z. L., J. Bai, and T. J. Cui, "Gradient index metamaterials realized by drilling hole arrays," *J. Phys. D*, Vol. 43, 055404–1–4, 2010, Doi: 10.1088/0022-3727/43/5/055404.

30. Kildishev, A. V. and V. M. Shalaev, "Engineering space for light via transformation optics," *Opt. Lett.*, Vol. 33, 43–45, 2008, Doi: 10.1364/OL.33.000043.
31. Li, J. and J. B. Pendry, "Hiding under the Carpet: A new strategy for cloaking," *Phys. Rev. Lett.*, Vol. 101, No. 20, 203901-1–4, 2008, Doi: 10.1103/PhysRevLett.101.203901.
32. Valentine, J., J. Li, T. Zentgraf, G. Bartal, and X. Zhang, "An optical cloak made of dielectrics," *Nat. Mater.*, Vol. 8, 568–571, 2009, Doi: 10.1038/nmat2461.
33. Liu, R., X. M. Yang, J. G. Gollub, J. J. Mock, T. J. Cui, and D. R. Smith, "Gradient index circuit by waveguided metamaterials," *Appl. Phys. Lett.*, Vol. 94, 073506-1–3, 2009, Doi: 10.1063/1.3081399.
34. Savini, G., P. A. R. Ade, and J. Zhang, "A new artificial material approach for flat THz frequency lenses," *Opt. Express*, Vol. 20, No. 23, 25766–25773, 2012, Doi: 10.1364/OE.20.025766.
35. Jain, S., M. Abdel-Mageed, and R. Mittra, "Flat-lens design using field transformation and its comparison with those based on transformation optics and ray optics," *IEEE Anten. Wirel. Propag. Lett.*, Vol. 12, 777–780, 2013, Doi: 10.1109/LAWP.2013.2270946.